Agr. Nat. Resour. 56 (2022) 287–298

AGRICULTURE AND NATURAL RESOURCES

Journal homepage: http://anres.kasetsart.org

Research article

Kinetic study of ethanol production from different sizes of two-step pretreated oil palm trunk by fed-batch simultaneous saccharification and fermentation

Imrana Niaz Sultan[a], Nongruk Khienpanya[a], Afrasiab Khan Tareen[a,c], Nicom Laemsak[b], Sarote Sirisansaneeyakul[a], Wirat Vanichsriratana[a], Pramuk Parakulsuksatid[a,*]

[a] *Department of Biotechnology, Kasetsart University, Bangkok, 10900, Thailand*

[b] *Department of Wood Technology, Faculty of Forestry, Kasetsart University, Bangkok, 10900, Thailand*

[c] *Department of Biotechnology, Faculty of Life Sciences and Informatics, BUITEMS, Quetta 87300, Pakistan*

Article Info

Article history:
Received 10 August 2021
Revised 28 January 2022
Accepted 2 February 2022
Available online 20 April 2022

Keywords:
Alkaline extraction,
Enzyme hydrolysis,
Oil palm trunk,
Particle size,
Simultaneous saccharification and fermentation

Abstract

Importance of the work: The particle size of lignocellulosic material exerts a significant impact on pretreatment and enzyme hydrolysis.

Objectives: To study the particle size impact of pretreated fibers on enzyme hydrolysis and ethanol production using simultaneous saccharification and fermentation (SSF).

Materials & Methods: In this study, oil palm trunk (OPT) chips were pretreated using a two-step pretreatment. The pretreated fibers of varied sizes (40 mesh, 40–60 mesh, 60 mesh and non-milled fibers) were used as substrates with different enzyme and substrate feeding approaches for efficient ethanol production based on SSF.

Results: The 40 mesh particles produced elevated levels of: ethanol concentration (C_P), 43.07 g/L; ethanol productivity (Q_P), 0.47 g/L/hr; ethanol yield ($Y_{P/S}$), 0.47 g/g; and ethanol theoretical yield, 90.26%. A further reduction in pretreated particle size from 40 mesh to 40–60 and 60 mesh significantly reduced the ethanol production and ethanol productivity rate. The highest Q_P rate in the log phase was observed with 40 mesh (0.994 g/L/hr), followed by non-milled fibers (0.809 g/L/hr). The optimized particle fibers (40 mesh) were further used for fed-batch SSF, which was carried out using four different sets of experiments. Each set was based on a strategy of feeding enzymes (celluase and β-glucosidase) and sterilized fibers.

Main finding: Out of studied sets of experiments, the strategy with enzymes fed at the start-up of fed-batch SSF and the addition of fibers at 12 hr, 24 hr and 36 hr produced a significantly higher ethanol concentration (41.65 g/L).

* Corresponding author.
E-mail address: fagipmp@ku.ac.th (P. Parakulsuksatid)

https://doi.org/10.34044/j.anres.2022.56.2.07

Introduction

Oil palm trunk (OPT) is a valuable lignocellulosic material that is readily available in Thailand, where oil palm plantations cover up to 10.2 million rai (1,632,000 ha) (Center for Applied Economic Research, 2017). The plantations are used for edible palm oil production and are replanted after 25–30 yr to maintain their economic life span and oil productivity (Woodham et al., 2019). The process of oil palm replantation causes immense agricultural waste that can be used for renewable energy and value-added industrial products (Tareen et al., 2020a).

Biofuels are generated from oil palm biomass owing to its higher cellulose content (Rezania et al., 2020). OPT, a lignocellulosic material, has three main components: cellulose, hemicelluloses and lignin that have a complicated arrangement and are recalcitrant to breakdown. However, the complex structure of the carbohydrates can be broken down into simpler components using efficient pretreatment (Baig, 2020), which improves the release of fermentable sugars (Wang et al., 2020).

Generally, there are limitations to pretreatment practices, including high operational expenses, corrosiveness to the appliances and toxicity. On the other hand, grinding and milling as physical pretreatment procedures are comparatively better than other types of pretreatments by primarily focusing on the diminution of particle size for potential and effective downstream processes, such as ethanol production (Rahmati et al., 2020).

Size reduction of biomass may improve the interactions between enzymes and cellulose, increase the avicel surface area and average molecular weight (Holland et al., 2018), which consequently improve the alteration of cellulose to monomers. Velmurugan and Muthukumar (2012) studied the influence of particle size of sugarcane bagasse for fermentable sugar production and observed that a smaller particle size of 0.27 mm produced a higher sugar yield of 96.27% than the average (0.91 mm) particle size. Yeh et al. (2010) observed significant improvement in the glucose concentration (60%) with a smaller particle size of 25.5 µm. Likewise, Rijal et al. (2014) reported that a smaller particle size (2 mm) significantly improved the rate of ethanol production in the first 24–48 hr. Milling of lignocellulosic fibers in a unit operation provides many advantages over non-milling fibers, including effective enzymatic hydrolysis, high sugar yield and ethanol concentrations (Yang et al., 2018). However, it can affect the suspension properties of fibers by increasing surface viscosity and mixing, thereby decreasing energy and mass transfers, in conjunction with the alteration of cellulose into glucose (Rahmati et al., 2020). Foremost, milling consumes a lot of energy so it can increase the production cost of ethanol (Talebnia et al., 2010).

Lignocellulosic ethanol can be produced using hydrolysis and fermentation that convert hemicellulose and cellulose to monomeric sugars followed by ethanol production (Wyman et al., 2019). Simultaneous saccharification and fermentation (SSF) involves both saccharification and fermentation in a single step. Compared to separate saccharification and fermentation (SHF), the SSF process has more benefits in terms of inhibiting the end product of β-glucosidase and only requiring a single reactor in the process. Furthermore, SSF is recommended over SHF owing to the overall ethanol yield requiring less time (Marulanda et al., 2019; Wilaithup et al., 2022).

Processing problems can be more easily addressed in fed-batch enzymatic hydrolysis by the gradual addition of enzyme and/or substrate, in order to avoid high viscosity (Sugiharto et al., 2016). Compared to conventional batch processes, the fed-batch enzymatic saccharification approach has many advantages in terms of reduced reactor volume and a minimum requirement of enzyme, which helps in reducing the overall investment cost (Jahnavi et al., 2017). Indeed, with a proper enzyme and substrate feeding strategy, it is the most advanced approach to achieve efficient ethanol concentration (Dey et al., 2020).

The current study aimed to observe the impact of different particle sizes of pretreated OPT fibers on enzyme hydrolysis and ethanol production using the SSF process. The study focused on the effects of different enzymes and substrate feeding approaches for efficient bioethanol production through an optimized SSF process.

Materials and Methods

Materials

Oil palm (*Elaeis guineensis* Jacq.) trunk (OPT) samples were bought from Plai Phraya district, Krabi province in southern Thailand. All chemicals were of analytical grade and were procured from Sigma-Aldrich. The chemicals consisted of: sodium hydroxide (98%); sulfuric acid (98%); sodium carbonate; sodium chloride; acetic acid; cellobiose (99%); ethanol (98%); glucose (99%); celluclast 1.5 L, cellulases and β-glucosidase (Novozym 188), The equipment consisted of a

steam explosion machine (Kumakai Nitto; Japan), sieves (425 µm and 250 µm), a vacuum pump (Eyela A-1000s; China), crucible pores, an ultraviolet-spectrophotometer (UV-1800; Shimadzu; Japan), a high-performance liquid chromatography unit (HPLC; A5333; Knaer; Germany) and a hot water bath (VS-1205S2W1; Vision Scientific Co. Ltd.; Thailand).

Pretreatment: Steam explosion, hot water extraction and alkaline extraction

The OPT samples were chopped into 20 mm × 20 mm × 5 mm chips using a wood chipper. Each batch of 150 g dry weight of chips was steam-exploded in a 10 L pressurized vessel at 210°C for 4 min, followed by hot water extraction for 30 min at 80°C with a solid-to-liquid ratio of 1:8. The blend of slurry and pulp was filtered to extract the hot fibers that were washed with tap water to neutralize the pH. Alkaline extraction was used for delignification of OPT fibers using 15% weight per volume (w/v) NaOH for 60 min at 90°C. After the alkaline extraction, the fibers were washed with tap water to obtain pH 7 and then placed in a hot-air oven at 80°C for drying (Tareen et al., 2021b). The compositional analysis of the OPT fibers was carried out using the given standard protocol of the Technical Association of the Pulp and Paper Industry (Tareen et al., 2021c).

Microorganisms and culture

Saccharomyces cerevisiae SC90 was cultured on yeast extract, peptone, dextrose medium containing: agar, 20 g/L; glucose, 20 g/L; peptone, 10 g/L; and yeast extract, 10 g/L for 48 hr at 30°C. An Erlenmeyer flask holding 30 mL yeast extract and peptone (YP) liquid medium (10 g/L yeast extract, 20 g/L glucose and 20 g/L peptone) was supplied with a single marginal colony of SC90 and incubated for 18 hr in a shaking incubator at 30°C at 150 revolutions per minute (rpm). Later, the starter culture was transferred to a 500 mL Erlenmeyer flask for fermentation.

Effect of particle size on enzyme hydrolysis of two-step pretreated oil palm trunk

The OPT fibers were subjected to enzyme hydrolysis with total weight of 10% (w/v). The cellulase enzyme loading was 15 filter paper unit (FPU)/g substrate and the enzyme activity assay was performed according to Selig et al. (2008). Novozym at 15 international units (IU)/g substrate was used to enhance the activity of β-glucosidase and analyzed using the assay technique of Berghem et al. (1976).

Enzymatic hydrolysis was performed with 10% dry weight of alkaline pretreated OPT fibers. For enzyme hydrolysis, the pretreated OPT fibers were processed in three different diameter sizes, namely 40 mesh (0.425 mm ≤ fibers ≤ 1.500 mm), 40–60 mesh (0.250 mm ≤ fibers ≤ 0.425 mm) and 60 mesh (fibers ≤ 0.25 mm), with non-milled pretreated fibers as the control. The fibers of each particle size were placed in separate Erlenmeyer flasks (500-mL) and buffered with 270 mL sodium citrate (0.05 M, pH 4.8). The enzymatic hydrolysis was performed at 40°C and 150 rpm using a water bath shaker for 96 hr. The hydrolysate samples were collected at 0 hr, 2 hr, 4 hr, 6 hr, 8 hr, 10 hr, 12 hr, 15 hr, 18 hr, 24 hr, 36 hr, 48 hr, 60 hr, 72 hr, 84 hr and 96 hr.

Effect of particle size on simultaneous saccharification and fermentation for ethanol production from two-step pretreated oil palm trunk fibers

For ethanol production, the SSF process was executed in 500 mL Erlenmeyer flasks, with each flask containing 300 mL YP media. One of the three different diameter sizes of OPT pretreated fibers and the non-milled fibers were added to separate flasks along with 10% starter culture, 15 FPU/g celluclast 1.5 L and 15 IU/g β-glucosidase simultaneously. The SSF fermentation with an initial pH of 4.8 was carried out in an incubator for 98 hr at 40°C and 150 rpm.

Fed-batch simultaneous saccharification and fermentation for ethanol production from two-step pretreated oil palm trunk fibers

Fed-batch SSF was performed in a 500 mL Erlenmeyer flask containing 300 mL YP media (pH 4.8). The 10% fibers of 40 mesh diameter were mixed with the sterilized liquid medium under standardized conditions (121°C for 15 min). The 10% starter culture was poured into an Erlenmeyer flask with similar amounts of enzymes as mentioned above for SSF (15 FPU/g celluclast 1.5 L enzyme and 15 IU/g β-glucosidase). Four different sets of experiments were carried out with final 10% substrate loadings, with each experiment using fed sterilized fibers and an enzyme feeding strategy: 1) the cellulase and β-glucosidase enzymes were supplemented at initiation of fed-batch SSF (fed fibers added twice at 12 hr, 24 hr and 36 hr); 2) the cellulase and β-glucosidase enzymes were added at the beginning of fed-batch SSF (fed fibers added

twice at 12 hr, 18 hr and 24 hr); 3) addition of one-quarter of the cellulase and β-glucosidase enzymes in the beginning and then equally at 12 hr, 24 hr and 36 hr of fermentation; and 4) one-quarter of the cellulase and β-glucosidase enzymes were added in the beginning, at then equally at 12 hr, 18 hr and 24 hr of fermentation. The experiment was carried out in an air-bath shaker for 98 hr at 40°C, with 150 rpm shaking (initial pH 4.8).

Analysis of cellobiose, glucose and ethanol

The standards of cellobiose, glucose and ethanol were separately prepared in deionized water and their concentrations were successfully determined using the HPLC equipped with an Aminex HPX-87P column. The column was eluted with 50 mM H_2SO_4 as the mobile phase at 50°C with a 0.6 mL/min flow rate (Xue et al., 2015).

Kinetic parameters for ethanol production

The standardized NREL protocol (Selig et al, 2008) was followed for the kinetic parameters of ethanol production based on Equations 1–8:

The cell production rate was based on Equation 1:

$$Q_x = \frac{X_t - X_0}{t - t_0} \quad (1)$$

where Q_x is the cell production rate (measured in log colony forming units (cfu) per liter per hour), X_0 is the initial cell concentration, X_t is the cell concentration at time t and t_0 is the initial time.

The glucose consumption rate (Q_S) (g/L/hr) is given in Equation 2:

$$Q_S = \frac{S_0 - S_t}{t - t_0} \quad (2)$$

where Q_S is the glucose consumption rate (measured in grams per liter per hour), S_0 is the initial glucose concentration, S_t: is glucose concentration at time t and t_0 is the initial time (hours).

The specific growth rate (μ) can be obtained by graphing the natural logarithm of the microbial cell intensity and time, where the slope of the graph in the exponential range is equal to the specific growth rate of microorganisms under the inoculation conditions according to the Equation 3:

$$\ln X_t = \ln X_0 + \mu X \quad (3)$$

where X is the concentration of microbial cells, X_0 is the initial concentration of microbial cells, X_t is the concentration of microbial cells at time t and μ is the specific growth rate.

The glucose specific consumption rate was calculated according to Equation 4:

$$q_s = \frac{1}{X}\left(\frac{dS}{dt}\right) = \frac{1}{\left(\frac{X_t + X_0}{2}\right)}\left(\frac{S_0 - S_t}{t - t_0}\right) \quad (4)$$

where q_s is the glucose specific consumption rate (measured in grams per log cfu per hour), S_0 is the initial glucose concentration, S_t is the glucose concentration at time t, X_0 is the initial cell concentration, X_t is the cell concentration at time t and t_0 is the starting time (hours).

The ethanol specific production rate was calculated using Equation 5:

$$q_p = \frac{1}{X}\left(\frac{dP}{dt}\right) = \frac{1}{\left(\frac{X_t + X_0}{2}\right)}\left(\frac{P_t - P_0}{t - t_0}\right) \quad (5)$$

where q_p is the ethanol specific production rate (measured in grams per log cfu per hour), P_0 is the initial ethanol concentration, P_t is the ethanol concentration at time t, X_0 is the initial cell concentration, X_t is the cell concentration at time t and t_0 is the starting time (hours).

The ethanol productivity was calculated using Equation 6:

$$Q_p\ (g/L/hr) = \frac{P_t - P_0}{t - t_0} \quad (6)$$

where Q_p is the ethanol productivity (measured in grams per liter per hour) P_0 is the ethanol titer at 0 hr (measured in grams per liter), P_t is the maximum ethanol titer (grams per liter), t_0 is the initial time (hours) and t is the time of the highest ethanol titer (hours).

The product yield coefficients ($Y_{P/S}$) were measured from the initial and final relevant concentrations in SSF method, using Equation 7:

$$Y_{p/s} = \frac{[P_t - P_0]}{f[\text{Biomass}]1.11} \quad (7)$$

where $Y_{P/S}$ is the product yield coefficient, P_t is the ethanol titer at the beginning (measured in grams per liter), P_0 is the maximum ethanol titer (grams per liter), *f* is the cellulose fraction of dry biomass, biomass is the OPT fibers (grams per liter) at the start and 1.11 is the theoretical yield conversion rate of cellobiose to glucose.

The ethanol theoretical yield was determined from the initial and final relevant concentrations during SSF using Equation 8:

$$Theoretical\ ethanol\ yield = \frac{/P_t - P_0/}{0.51f/Biomass/1.11} \times 100 \quad (8)$$

where 0.51 is the theoretical value to convert glucose to ethanol (Tareen et al., 2021b).

Statistical analysis

Analysis of variance and Fisher's least significant difference test (SAS version 8.01) were used to identify statistically significant differences in ethanol concentration, ethanol yield, ethanol productivity and theoretical ethanol yield. Differences were considered significant at $p < 0.05$.

Results and discussion

Compositional analysis of oil palm trunk fibers

Prior to pretreatment, the chemical composition of OPT was: 11.42% extractive substances, 77.01% holocellulose, 39.65% cellulose, 23.03% pentosan, 23.47% lignin and 1.46% ash on dry weight basis. However, owing to steam explosion followed by hot water washing and alkaline extraction, the content of holocellulose and cellulose increased to 89.41% and 77.59%, respectively. Additionally, the percentage quantity of pentosan, lignin and ash dropped to 1.73%, 9.80% and 0.52%, respectively. These results were similar to those reported by Tareen et al. (2021b) who managed to extract 87.89% of holocellulose from OPT fibers after alkaline pretreatment. Likewise, Tareen et al. (2020b) reported 73.96% cellulose and a significant amount of lignin was reduced to 11.68% from OPT fibers using alkaline hydrogen peroxide pretreatment.

Effect of particle size on enzyme hydrolysis of two-step pretreated oil palm trunk fibers

The milled (with varying particle sizes) and non-milled (control) pretreated OPT fibers were subjected to enzymatic hydrolysis. The use of milled fibers led to elevated levels of glucose, which caused a higher ethanol concentration. Conversely, higher enzymatic hydrolysis resisted stirring of the fermentation medium, resulting in end-product inhibition. Table 1 shows the glucose concentrations and conversions from different particle sizes. The total glucose released from the control fibers was 83.37 g/L with glucose conversion of 94.37%. A significant increase was observed in the glucose concentration and glucose conversion (87.36 g/L and 98.88%, respectively) when the particle size was reduced to 40 mesh. However, a further reduction in particle size significantly decreased the total glucose release and conversion (to 77.24 g/L glucose concentration and 87.81% glucose conversion for 40–60 mesh and to 72.89 g/L glucose concentration and 82.46% glucose conversion for 60 mesh), as shown in Table 1. Similar findings were reported by Fernandes et al. (2020) who observed better enzyme action at 0.425 mm (35 mesh) of sugarcane bagasse particles that augmented the glucose yield. Additionally, Alves et al. (2020) reported a 20% increase in the glucose yield when the particle size of sugarcane bagasse was reduced from 30 mesh to 40 mesh; however, a further decrease in the particle size did not significantly improve the glucose yield. The particle size influences the chemical and structural properties of lignocellulosic material; the smaller the particle size, the lower the amount of cellulose (Neto et al., 2016). The chemical changes have been attributed to the formation of abundant co-products, such as furfural and hydroxymethylfurfural (Nagarajan et al., 2021). In addition, structural changes in different particle sizes play a vital role in strengthening cellulose, which leads to functional group modifications in cellulose and hemicellulose (Bandikari et al., 2014). Furthermore, a smaller particle size results in higher specific surface area for enzyme hydrolysis but this also depends on the size and shape of pores (Lu et al., 2019). The pore size, volume and shape in cellulose and the accessibility of enzymes can highly influence the enzymatic hydrolysis of lignocellulosic biomass (Herbaut et al., 2018). Nonetheless, further milling of particles to a smaller size decreased the number of pores (Nagarajan et al., 2021) and enhanced viscosity, that increased the difficulty of product transfer resistance (Ran et al., 2012), increased the production of high amounts of inhibitory compounds and the formation of pseudo-lignin, resulting in lower enzymatic hydrolysis (Kapoor et al., 2019).

Table 1 Glucose concentration and conversion levels for different sizes of two-step pretreated oil palm trunk fibers

Particle size (mesh)	Glucose concentration (g/L)	Conversion (%)
Control	83.37±2.12[b]	94.37±3.01[b]
40 mm	87.36±1.87[a]	98.88±2.16[a]
40–60 mm	77.24±2.75[c]	87.81±1.98[c]
60 mm	72.85±1.91[d]	82.46±2.42[d]

[a–d] Values (mean ± SD) within same column with different lowercase superscripts are significantly ($p < 0.05$) different

Effect of particle size on simultaneous saccharification and fermentation for ethanol production from two-step pretreated oil palm trunk fibers

The SSF process was performed with different sizes of OPT fiber particles to produce ethanol. During the SSF fermentation of non-milled fibers, the glucose concentration abruptly increased at the commencement of fermentation but rapidly decreased within 12 hr. The maximal strength of viable cells at 36 hr eventually dropped after incubation for 48 hr. The initial ethanol concentration at 6 hr and at the end of fermentation period (96 hr) was 39.85 g/L (Fig. 1A). In addition, the kinetic parameters of growth and ethanol production could be separated into the log phase, stationary phase and death phase. The kinetic parameters—live cells concentration, ethanol concentration (C_P), glucose consumption rate (Q_S), ethanol production rate (Q_P), glucose specific consumption rate (q_S) and ethanol specific production rate (q_P) were calculated using Equations 1–8 in all three phases. The live cells concentration in the log and stationary phases (11.269 log cfu/L and 11.326 log cfu/L, respectively) were almost similar and followed by a slight decrease in the death phase (10.678 log cfu/L). The ethanol concentration gradually rose from 27.699 g/L in the log phase to 30.245 g/L in the stationary phase and then rose to 39.845 g/L in the death phase. The log phase of non-milled fibers lasted until 24 hr of SSF and had higher rates of Q_S and Q_P (2.324 g/L and 0.809 g/L/hr, respectively) that indicated the utilization of glucose for ethanol production (Table 2).

Fig. 1B shows that the glucose concentration in SSF fermentation with 40 mesh, increased immediately from the initiation of fermentation but decreased after 36 hr. A similar pattern was observed for the ethanol concentration, which increased in the first 24 hr, while the strength of viable cells improved after 18 hr. The final ethanol titer obtained after 84 hr of SSF was 43.07 g/L. The live cells concentration in the growth and ethanol production stages using 40 mm-sized particles were almost similar in all three phases. The log and stationary phases of the 40 mesh fibers each lasted until 24 hr in SSF, which was the longest of all the stationary phases for the studied fibers. The maximum Q_P value was observed with 40 mesh in the log and death phases (0.994 g/L/hr and 0.372 g/L/hr, respectively). In addition, similar sized particle fibers produced a significantly higher ethanol concentration and q_P of 43.074 g/L and 0.095 g/ log cfu/h, respectively (Table 3). These results were better than those reported by Rorke et al. (2017) who recorded an ethanol production rate of 0.52 g/L/hr using waste sorghum leaves.

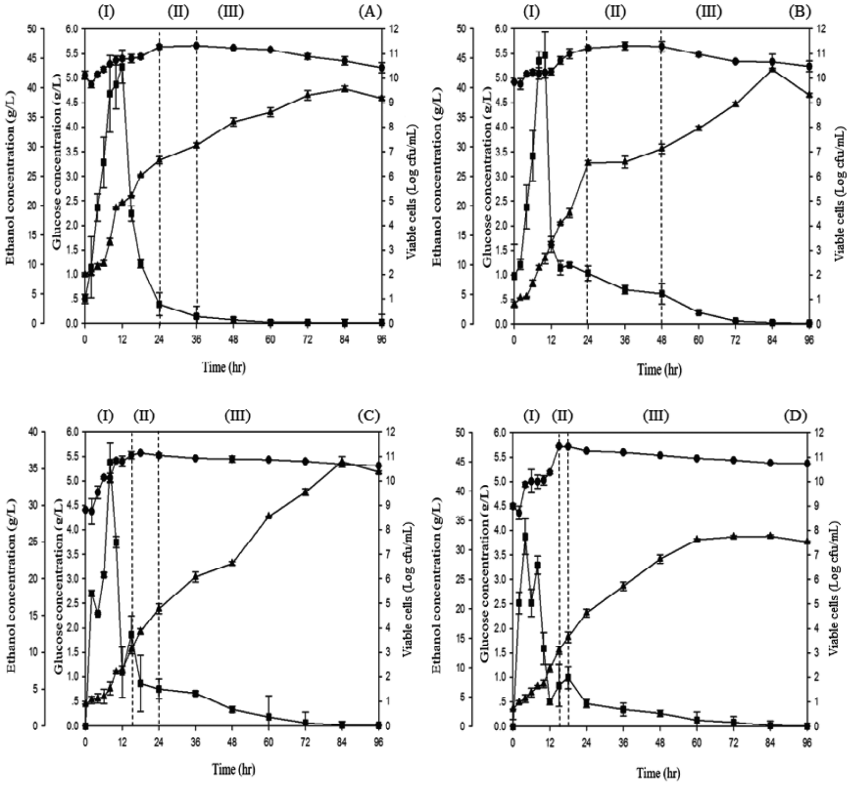

Fig. 1 Simultaneous saccharification and fermentation with 10% (weight per volume) substrate loading using different particle sizes: (A) non-milling fiber as control; (B) 40 mesh; (C) 40–60 mesh; (D) 60 mesh, where ■ = glucose, ● = viable cells, ▲ = ethanol, I, II, and III indicate log, stationary and death phases, respectively, cfu = colony forming units and error bars indicate ± SD

Table 2 Kinetic parameters of growth and ethanol production of non-milled size oil palm trunk fibers (control) for simultaneous saccharification and fermentation

Parameter	Unit	Log phase	Stationary phase	Death phase
Time	hr	0–24	24–36	36–96
Live cells concentration	log cfu/L	11.269	11.326	10.678
Ethanol concentration (C_P)	g/L	27.699	30.245	39.845
Cell production rate (Q_X)	log cfu/L/hr	0.049	0.005	0
Glucose consumption rate (Q_S)	g/L/hr	2.124	0.416	0.450
Ethanol production rate (Q_P)	g/L/hr	0.809	0.212	0.20
Specific growth rate (μ)	μ/hr	0.004	0	-
Specific death rate (K_d)	K_d/hr	-	-	0.001
Glucose specific consumption rate (q_S)	g/ log cfu/hr	0.218	0.037	0.041
Ethanol specific production rate (q_P)	g/ log cfu/hr	0.076	0.015	0.018
Live cell yield ($Y_{X/S}$)	log cfu/g	0.021	0.017	0
Ethanol yield ($Y_{P/S}$)	(g/g)	0.348	0.510	0.445

Table 3 Kinetic parameters of growth and ethanol production of 40 mesh size oil palm trunk fibers for simultaneous saccharification and fermentation

Parameter	Unit	Log phase	Stationary phase	Death phase
Time	hr	0–24	24–48	48–96
Live cells concentration	log cfu/L	11.180	11.258	11.016
Ethanol concentration (C_P)	g/L	18.757	29.692	43.074
Cell production rate (Q_X)	log cfu/L/hr	0.064	0.002	0
Glucose consumption rate (Q_S)	g/L/hr	2.316	0.692	0.442
Ethanol production rate (Q_P)	g/L/hr	0.994	0.102	0.372
Specific growth rate (μ)	μ/hr	0.01	0	-
Specific death rate (K_d)	K_d/hr	-	-	0.002
Glucose specific consumption rate (q_S)	g/ log cfu/hr	0.212	0.062	0.041
Ethanol specific production rate (q_P)	g/ log cfu/hr	0.095	0.009	0.034
Live cell yield ($Y_{X/S}$)	log cfu/g	0.028	0.003	0
Ethanol yield ($Y_{P/S}$)	(g/g)	0.448	0.147	0.840

The SSF process with 40–60 mesh had a reduced glucose concentration after 24 hr, though it increased initially with the exponential growth of viable cells after 8 hr. Additionally, the ethanol concentration was enhanced in the first 24 hr period and the maximal quantity achieved was 35.95 g/L (Fig. 1C). The kinetic parameters of growth and ethanol production in SSF were studied for 40–60 mesh particles. The live cells concentration remained almost similar in all three phases, yet Q_P and $Y_{P/S}$ were higher in the stationary phase (0.795 g/L/hr and 0.959 g/g, respectively). In contrast to the other particle sizes, the 40-60 mesh fibers had the highest Q_S value of 2.495 g/L/hr (Table 4) in the log phase which gradually reduced from 0.829 g/L/hr in the stationary phase to 0.507 g/L/hr in the death phase, followed by the 40 mesh particle size with a Q_S value of 2.316 g/L/hr. The highest glucose specific consumption rate (q_S) of 0.252 g/ log cfu/h was in log phase of the 40–60 mesh particle size fibers, though this decreased significantly to 0.075 g/log cfu/hr in the stationary phase and reached 0.047 g/log cfu/hr in the death phase (Table 4). Nevertheless, there were no significant differences among the q_S values for all the studied fiber particle sizes.

In the 60 mesh SSF process, the concentration of glucose started decreasing after 24 hr and an increase in viable cells was measured after 12 hr. The ethanol concentration started to increase in the first 24 hr and reached 32.35 g/L at its peak (Fig. 1D). The kinetic parameters during the SSF process for ethanol production with 60 mm-sized particles had the shortest stationary phase (4 hr), and the longest death phase (78 hr), as shown in Table 5. The concentrations of live cells were almost similar in the log and stationary phases but reduced in the death phase. The maximum increase C_P (from 19.296 g/L to 32.352 g/L) was in the death phase of the 60 mm-sized particles. Q_P was 0.616 g/L/hr in the log phase, which increased to 0.706 g/L/hr in the stationary phase but then reduced to 0.218 g/L/hr in the death phase. Surprisingly, the shortest stationary phase produced the highest ethanol yield ($Y_{P/S}$) of 0.977 g/g. Compared to the other studied particles, q_P for the 60 mm-sized particles did not reduce and remained almost similar in the log and stationary phases (Table 5).

Table 4 Kinetic parameters of growth and ethanol production of 40–60 mesh size oil palm trunk fibers for simultaneous saccharification and fermentation

Parameter	Unit	Log phase	Stationary phase	Death phase
Time	hr	0–15	15–24	24–96
Live cells concentration	log cfu/L	11.051	11.039	10.685
Ethanol concentration (C_P)	g/L	12.527	19.679	35.946
Cell production rate (Q_X)	log cfu/L/hr	0.149	-0.001	0
Glucose consumption rate (Q_S)	g/L/hr	2.495	0.829	0.507
Ethanol production rate (Q_P)	g/L/hr	0.627	0.795	0.310
Specific growth rate (μ)	μ/hr	0.02	0	-
Specific death rate (K_d)	K_d/hr	-	-	0.001
Glucose specific consumption rate (q_S)	g/log cfu/hr	0.252	0.075	0.047
Ethanol specific production rate (q_P)	g/log cfu/hr	0.063	0.072	0.029
Live cell yield ($Y_{X/S}$)	log cfu/g	0.060	0	0
Ethanol yield ($Y_{P/S}$)	(g/g)	0.251	0.959	0.612

Table 5 Kinetic parameters of growth and ethanol production of 60 mesh size oil palm trunk fibers for simultaneous saccharification and fermentation

Parameter	Unit	Log phase	Stationary phase	Death phase
Time	hr	0–15	15–18	18–96
Live cells concentration	log cfu/L	11.429	11.250	10.757
Ethanol concentration (C_P)	g/L	12.946	19.296	32.352
Cell production rate (Q_X)	log cfu/L/hr	0.162	-0.02	0
Glucose consumption rate (Q_S)	g/L/hr	2.211	0.722	0.491
Ethanol production rate (Q_P)	g/L/hr	0.616	0.706	0.218
Specific growth rate (μ)	μ/hr	0.02	0	-
Specific death rate (K_d)	K_d/hr	-	-	0.001
Glucose specific consumption rate (q_S)	g/log cfu/hr	0.218	0.064	0.045
Ethanol specific production rate (q_P)	g/log cfu/hr	0.066	0.062	0.017
Live cell yield ($Y_{X/S}$)	log cfu/g	0.073	-0.028	0
Ethanol yield ($Y_{P/S}$)	(g/g)	0.301	0.977	0.443

This study involved the investigation of milled fibers of different diameters, using non-milled fibers as the control to investigate obtaining elevated concentrations of ethanol. The results are displayed in Table 6. The 40 mesh-sized fibers produced significantly greater values for ethanol concentration (43.07 g/L), ethanol yield (0.47 g/g), ethanol theoretical yield (90.26%) and ethanol productivity (0.47 g/L/hr). There was a significantly lower ethanol concentration produced from the control fibers (39.85 g/L), resulting in 0.40 g/L/hr ethanol productivity, 0.46 g/g ethanol yield and 87.74% ethanol theoretical yield. In contrast, the 40–60 mesh particles produced ethanol at 35.95 g/L concentration, 0.39 g/L/hr productivity, 0.39 g/g yield and 75.08% theoretical yield. The ethanol concentration, ethanol productivity, ethanol yield and ethanol theoretical yield obtained using the 60 mesh particles were 32.35 g/L, 0.36 g/L/hr, 0.34 g/g and 66.88%, respectively. The simultaneous saccharification and fermentation process carries out the saccharification and fermentation by yeast in a single fermenter. SSF is the most commonly recommended process due to the use of inexpensive agricultural residues for cost effective ethanol production at an industrial scale (Kanagasabai et al., 2019). The enzymatic hydrolysis increases the surface area by reducing the particle size and crystallinity due to the milling pretreatment (Jiang et al., 2016). Nevertheless, a reduction in particle size exerts an adverse effect by increasing the viscosity and reducing

Table 6 Comparison of oil palm trunk pretreated particles of various mesh sizes for ethanol production

Particle size (mesh)	Ethanol concentration (g/L)	Ethanol productivity (g/L/hr)	Ethanol yield (g/g)	Theoretical ethanol yield (%)
Control	39.85±1.09^{b}	0.40±0.41^{b}	0.46±0.28^{a}	87.74±1.65^{a}
40	43.07±0.62^{a}	0.47±0.12^{a}	0.47±0.16^{a}	90.26±0.43^{a}
40–60	35.95±0.92^{c}	0.39±0.23^{ab}	0.39±0.22^{b}	75.08±1.56^{b}
60	32.35±1.28^{d}	0.36±0.58^{c}	0.34±0.13^{c}	66.88±1.02^{c}

Values (mean ± SD) within the same column with different lowercase superscripts are significantly ($p < 0.05$) different

the inter-particle distance, resulting in decreases in aeration, metabolism and the growth of microorganisms (Wan and Li, 2010; Jiang et al., 2016). Conversely, some studies reported a diminution in viscosity and yield stress with a smaller particle size as the lessened fiber macropores led to lower water restraining proficiency (da Silva et al., 2020).

Fed-batch simultaneous saccharification and fermentation for ethanol production from two-step pretreated oil palm trunk fibers

Fed-batch SSF of OPT fibers was carried out for ethanol production with 10% final dry solid loading. Fig. 2 shows the levels of viable cells, glucose, cellobiose and ethanol concentration during the fermentation process. The glucose concentration elevated rapidly at the beginning of SSF and was depleted after 84 hr. The cellobiose concentration reached its maximum at 24 hr, but was depleted after 72 hr. There was an increase in viable cells after 12 hr. At the end of the fed-batch fermentation period (96 hr) the ethanol concentration was 41.65 g/L. Fig. 3 shows that the viable cells reached the maximum level at 24 hr but reduced after 36 hr. At initial incubation (2 hr), glucose concentrations quickly improved but reduced after 72 hr. The cellobiose concentration reached its maximum at 2 hr but declined before 84 hr. The maximum ethanol concentration was 38.35 g/L. Fig. 4 shows that the cellobiose concentration increased quickly in the beginning but was depleted after 24 hr. The glucose concentration reached its maximum at 6 hr and reduced after 72 hr. The strength of viable cells reached its peak at 24 hr but declined after 36 hr. Before 24 hr, glucose was utilized to produce yeast cells and after 24 hr it was converted to ethanol. The experimental results revealed that ethanol production was initiated from the beginning of fermentation and reached its maximum (39.72 g/L) after 72 hr. Fig. 5 shows that the glucose concentration increased from the beginning of the SSF process and was depleted after 60 hr of incubation. Before 24 hr, glucose was used for cell growth but afterward, it was converted to ethanol having (38.21 g/L).

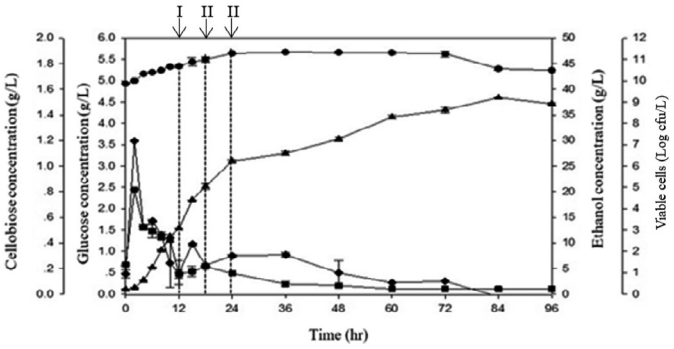

Fig. 3 Effect of substrate and cellulase feeding strategy in fed-batch simultaneous saccharification and fermentation (celluase and β-glucosidase enzymes added at start-up), with 10% solid loading at 12 hr, 18 hr and 24 hr for 40 mesh-sized particles, where ■ = glucose, ● = viable cells, ♦ = cellobiose, ▲ = ethanol, cfu = colony forming units and error bars indicate ± SD

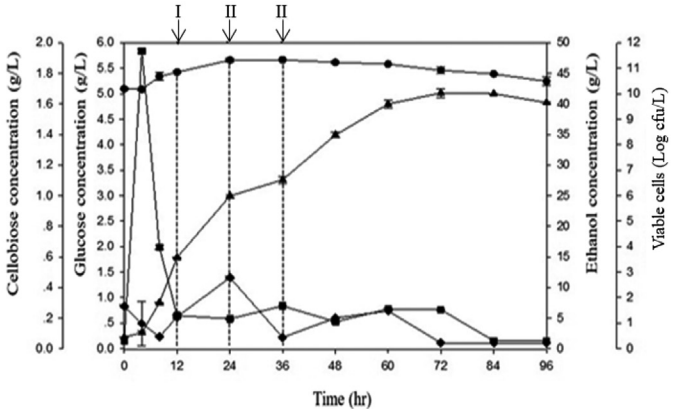

Fig. 2 Effect of substrate and cellulase feeding strategy in fed-batch simultaneous saccharification and fermentation (celluase and β-glucosidase enzymes added at start-up), with 10% solid loading at 12 hr, 24 hr and 36 hr for 40 mesh-sized particles, where ■ = glucose, ● = viable cells, ♦ = cellobiose, ▲ = ethanol, cfu = colony forming units and error bars indicate ± SD

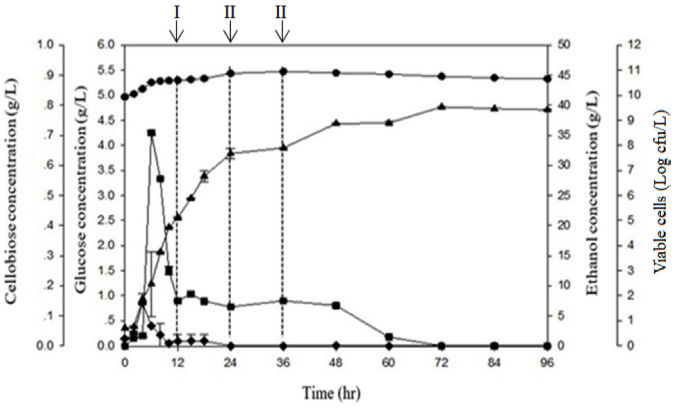

Fig. 4 Effect of substrate and cellulase feeding strategy in fed-batch simultaneous saccharification and fermentation, with addition of one-quarter of celluase and β-glucosidase enzymes equally at beginning, 12 hr, 24 hr and 36 hr of fermentation, with 10% solid loading from 40 mesh-sized particles, where ■ = glucose, ● = viable cells, ♦= cellobiose, ▲ = ethanol, cfu = colony forming units and error bars indicate ± SD

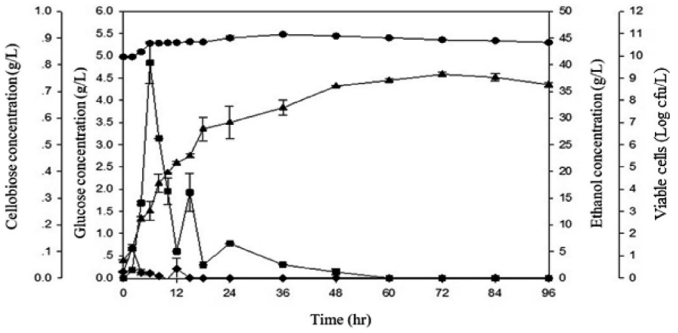

Fig. 5 Effect of substrate and cellulase feeding strategy in fed-batch simultaneous saccharification and fermentation. Addition of one-quarter of celluase and β-glucosidase enzymes equally at beginning, 12 hr, 18hr and 24 hr of fermentation, with 10% solid loading for 40 mesh-sized particles, where ■ = glucose, ● = viable cells, ♦= cellobiose, ▲ = ethanol, cfu = colony forming units and error bars indicate ± SD

To increase ethanol concentration, four varied substrate and enzyme feeding strategies were studied: 1) celluase and β-glucosidase enzymes added at the beginning of fed-batch SSF (addition of fed fibers twice at 12 hr, 24 hr and 36 hr); 2) celluase and β-glucosidase enzymes added at the beginning of fed-batch SSF (twice at 12 hr, 24 hr and 36 hr); 3) addition of one-quarter of celluase and β-glucosidase enzymes equally at the beginning, 12 hr, 24 hr and 36 hr of fermentation; and 4) one-quarter of celluase and β-glucosidase enzymes added equally at the start, 12 hr, 18 hr and 24 hr of fermentation. The results displayed in Table 7 reveal that the controlled fibers produced elevated ethanol concentration levels of 43.07 g/L, 0.47 g/L/hr ethanol productivity, 0.47 g/g ethanol yield, and 90.26% theoretical ethanol yield. However, Batch 1 had 0.55 g/L/hr ethanol productivity, 41.65 g/L ethanol concentration, 0.46 g/g ethanol yield and 90.50% theoretical ethanol yield. The ethanol concentration was higher compared to the study by Bedzo et al. (2021) who produced 39 g/L of ethanol with 82% of theoretical ethanol using sweet sorghum bagasse in fed batch SSF. Although the ethanol concentration of Batch 1 was less than that of the control ($p < 0.05$), the ethanol productivity of Batch 1 was higher than that of control ($p < 0.05$). Notably, the shorter time of around 12 hr might lead to a reduction in the operating cost of ethanol production. In addition, there were no significant differences between Batch 1 and the control in the efficiency of conversion from fiber to ethanol, ethanol yield and theoretical ethanol yield. Hoyer et al. (2010) also suggested the addition of all the enzymes into a fermenter at the beginning of fed-batch SSF. A similar pattern of adding all the cellulase enzymes at the initiation of fermentation was followed by Zhao et al. (2013) and Tareen et al. (2021a), with both studies reporting that this produced the highest glucose concentration. The maximal ethanol production of Batch 3 was 39.72 g/L ethanol concentration, 0.51 g/L/hr ethanol productivity, 0.43 g/g ethanol yield and 85.07% theoretical ethanol yield, whereas Batch 4 produced 38.21 g/L ethanol concentration with ethanol productivity of 0.49 g/L/hr, an ethanol yield of 0.41 g/g and 79.55% theoretical ethanol yield.

This study primarily focused on the influence of the particle size of the OPT fibers in the range 40–60 mesh compared to non-milled pretreated fibers for ethanol production. The results indicated that an OPT particle size of 40 mesh produced the highest ethanol concentration (43.07 g/L) for the SSF process. However, the fed-batch SSF strategy consisted of using optimized particle size (40 mesh) fibers and all the celluase and β-glucosidase enzymes being added at start-up (fed fibers added at 12 hr, 24 hr and 36 hr); this produced the highest ethanol concentration of 41.65 g/L. Therefore, the fed-batch SSF process utilizing milled OPT fibers has the potential to increase bioethanol production.

Table 7 Comparison of different substrate at 10% (weight per volume) substrate loading and enzyme feeding of pretreated oil-palm trunk fibers for ethanol production

Particle size (mesh)	Ethanol concentration (g/L)	Ethanol productivity (g/L/hr)	Ethanol yield (g/g)	Theoretical ethanol yield (%)
Control	43.07±0.62^{a}	0.47±0.12^{bc}	0.47±0.16^{a}	90.26±0.43^{a}
Batch 1	41.65±1.43^{b}	0.55±0.28^{a}	0.46±0.21^{a}	90.50±0.51^{a}
Batch 2	38.35±1.76^{c}	0.45±0.75^{d}	0.43±0.29^{b}	85.07±0.72^{b}
Batch 3	39.72±1.57^{c}	0.51±0.41^{b}	0.43±0.33^{b}	85.07±0.65^{b}
Batch 4	38.21±0.93^{c}	0.49±0.33^{bc}	0.41±0.29^{c}	79.55±0.23^{c}

Values (mean ± SD) within the same column with different lowercase superscripts are significantly ($p < 0.05$) different

Batch 1 = addition of enzymes at start of fed-batch simultaneous saccharification and fermentation (SSF), with fed fibers added at 12 hr, 24 hr and 36 hr); Batch 2 = addition of enzymes at beginning of fed-batch SSF, with fed fibers added at 12 hr, 18 hr and 24 hr; Batch 3 = addition of one-quarter of enzymes added equally at beginning, 12 hr, 24 hr and 36 hr of fermentation; Batch 4 = addition of one-quarter of enzymes at beginning, 12 hr, 18 hr and 24 hr of fermentation

Conflict of Interest

The authors declare that there are no conflicts of interest.

Acknowledgements

Funding was provided by the Kasetsart University Research and Development Institute (KURDI), Bangkok, Thailand. Support was provided by the Department of Biotechnology, Faculty of Agro-Industry, Kasetsart University, Thailand.

References

Alves, R.C., Melati, R.B., Casagrande, G.M.S., Contiero, J., Pagnocca, F.C., Brienzo, M. 2020. Sieving process selects sugarcane bagasse with lower recalcitrance to xylan solubilization. J. Chem. Technol. Biot. 96: 327–334. doi.org/10.1002/jctb.6541

Baig, K.S. 2020. Interaction of enzymes with lignocellulosic materials: Causes, mechanism and influencing factors. Bioresour. Bioprocess. 7: 21. doi.org/10.1186/s40643-020-00310-0

Bandikari, R., Poondla, V., Obulam, V.S.R. 2014. Enhanced production of xylanase by solid state fermentation using *Trichoderma koeningi* isolate: Effect of pretreated agro-residues. 3 Biotech 4: 655–664. doi.org/10.1007/s13205-014-0239-4

Bedzo, O.K.K., Dreyer, C.B., Rensburg, E.V., Görgens, J.F. 2021. Optimisation of pretreatment catalyst, enzyme cocktail and solid loading for improved ethanol production from sweet sorghum bagasse. Bioenerg. Res. 2021: 1–13 doi.org/10.1007/s12155-021-10298-w

Berghem, L.E., Pettersson, L., Axiö-fredriksson, U. 1976. The mechanism of enzymatic cellulose degradation. Purification and some properties of two different 1,4beta-glucan glucanohydrolases from *Trichoderma viride*. Eur. J. Biochem. 61: 621–630.

Center for Applied Economic Research. 2017. Study Project for Development of Oleochemical Industrial from Palm Oil. Office of Industrial Economics, Ministry of Industry. Bangkok, Thailand.

da Silva, A.S., Espinheira, R.P., Teixeira, R.S.S., Souza, M.F., de Ferreira-Leitão, V., Bon, E.P.S. 2020. Constraints and advances in high-solids enzymatic hydrolysis of lignocellulosic biomass: A critical review. Biotechnol. Biofuels 13: 58. doi.org/10.1186/s13068-020-01697-w

Dey, P., Pal, P., Kevin, J., Das, D. 2020. Lignocellulosic bioethanol production: Prospects of emerging membrane technologies to improve the process – A critical review. Rev Chem. Eng. 36: 333–367. doi.org/10.1515/revce-2018-0014

Fernandes, E.S., Danilo, B., Fernando, C.P., Brienzo, M. 2020. Minor biomass particle size for an efficient cellulose accessibility and enzymatic hydrolysis. ChemistrySelect 5: 7627–7631. doi.org/10.1002/slct.202001008

Herbaut, M., Zoghlami, A., Habrant, A., Falourd, X., Foucat, L., Chabbert, B., Paës, G. 2018. Multimodal analysis of pretreated biomass species highlights generic markers of lignocellulose recalcitrance. Biotechnol. Biofuels. 11: 52. doi.org/10.1186/s13068-018-1053-8

Holland, S., Foster, T., MacNaughtan, W., Tuck, C. 2018. Design and characterisation of food grade powders and inks for microstructure control using 3D printing. J. Food Eng. 220: 12–19. doi.org/10.1016/j.jfoodeng.2017.06.008

Hoyer, K., Galbe, M., Zacchi, G. 2010. Effects of enzyme feeding strategy on ethanol yield in fed-batch simultaneous saccharification and fermentation of spruce at high dry matter. Biotechnol. Biofuels. 3: 14. doi.org/10.1186/1754-6834-3-14

Jahnavi, G., Prashanthi, G.S., Sravanthi, K., Rao, L.V. 2017. Status of availability of lignocellulosic feed stocks in India: Biotechnological strategies involved in the production of bioethanol. Renew. Sust. Energ. Rev. 73: 798–820. doi.org/10.1016/j.rser.2017.02.018

Jiang, J., Wang, J., Zhang, X., Wolcott, M. 2016. Evaluation of physical structural features on influencing enzymatic hydrolysis efficiency of micronized wood. RSC Adv. 6: 103026–103034. doi.org/10.1039/C6RA22371K

Kapoor, M., Semwal, S., Satlewal, A., Christopher, J., Gupta, R.P., Kumar, R., Puri, S.K., Ramakumar, S.S.V. 2019. The impact of particle size of cellulosic residue and solid loadings on enzymatic hydrolysis with a mass balance. Fuel 245: 514–520. doi.org/10.1016/j.fuel.2019.02.094

Kanagasabai, M., Maruthai, K., Thangavelu, V. 2019. Simultaneous saccharification and fermentation and factors influencing ethanol production in SSF process. In: Yun, Y. (Ed.). Alcohol Fuels. IntechOpen. London, UK, pp. 1–13.

Lu, M., Li, J., Han, L., Xiao, W. 2019. An aggregated understanding of cellulase adsorption and hydrolysis for ball-milled cellulose. Bioresour. Technol. 273: 1–7. doi.org/10.1016/j.biortech.2018.10.037

Marulanda, V.A., Gutierrez, C.D.B., Alzate, C.A.C. 2019. Thermochemical, biological, biochemical, and hybrid conversion methods of bio-derived molecules into renewable fuels. In: Hosseini, M. (Ed.). Advanced Bioprocessing for Alternative Fuels, Biobased Chemicals, and Bioproducts. Woodhead Publishing. Sawston, Cambridge, UK, pp. 59–81.

Nagarajan, A., Thulasinathan, B., Arivalagan, P., Alagarsamy, A., Muthuramalingam, J.B., Thangarasu, S.D., Thangavel, K. 2021. Particle size influence on the composition of sugars in corncob hemicellulose hydrolysate for xylose fermentation by *Meyerozyma caribbica*. Bioresour. Technol. 340: 125677. doi.org/10.1016/j.biortech.2021.125677

Neto, F.S.P.P., de Lucca, E.A., Masarin, F. 2016. Particle size influence on the chemical composition from waste *Eucalyptus* in the processing for industrial production of cellulose pulp. Chem. Eng. Trans. 50: 337–342. doi: 10.3303/CET1650057

Rahmati, S., Doherty, W., Dubal, D., Atanda, L., Moghaddam, L., Sonar, P., Hessel, V., Ostrikov, K. 2020. Pretreatment and fermentation of lignocellulosic biomass: Reaction mechanisms and process engineering. React. Chem. Eng. 5: 2017–2047. doi.org/10.1039/D0RE00241K

Ran, Y., Wang, Y.Z., Liao, Q., Zhu, X., Chen, R., Lee, D.J., Wang, Y.M. 2012. Effects of operation conditions on enzymatic hydrolysis of high-solid rice straw. Int. J. Hydrogen Energ. 37: 13660–13666. doi.org/10.1016/j.ijhydene.2012.02.080

Rezania, S., Oryani, B., Cho, J., Sabbagh, F., Rupani, P.F., Talaiekhozani, A., Rahimi, N., Ghahroud, M.L. 2020. Technical aspects of biofuel production from different sources in Malaysia—A Review. Processes 8: 993. doi.org/10.3390/pr8080993

Rijal, B., Biersbach, G., Gibbons, W., Pryor, S. 2014. Effect of initial particle size and densification on AFEX-pretreated biomass for ethanol production. Appl. Biochem. Biotechnol. 174: 845–854. doi.org/10.1007/s12010-014-1120-y

Rorke, D.C.S., Kana, E.B.G. 2017. Kinetics of bioethanol production from waste sorghum leaves using *Saccharomyces cerevisiae* BY4743. Fermentation 3: 19. doi.org/10.3390/fermentation3020019

Selig, M., Weiss, N., Ji, Y. 2008. Enzymatic Saccharification of Lignocellulosic Biomass; Laboratory Analytical Procedure (LAP). National Renewable Energy Laboratory Technical Report, NREL/TP510-42629. Golden CO, USA.

Sugiharto, Y.E., Harimawan, A., Kresnowati, M.T., Purwadi, R., Mariyana, R., Fitriana, A.H., Hosen, H.F. 2016. Enzyme feeding strategies for better fed-batch enzymatic hydrolysis of empty fruit bunch. Bioresour. Technol. 207: 175–179. doi.org/10.1016/j.biortech.2016.01.113

Talebnia, F., Karakashev, D., Angelidaki, I. 2010. Production of bioethanol from wheat straw: An overview on pretreatment, hydrolysis and fermentation. Bioresour. Technol. 101: 4744–4753. doi.org/10.1016/j.biortech.2009.11.080

Tareen, A.K., Punsuvon, V., Sultan, I.N., Khan, M.W., Parakulsuksatid, P. 2021a. Cellulase addition and pre-hydrolysis effect of high solid fed-batch simultaneous saccharification and ethanol fermentation from a combined pretreated oil palm trunk. ACS Omega 6: 26119–26129. doi.org/10.1021/acsomega.1c03111

Tareen, A.K., Sultan, I., Songprom, K., Laemsak, N., Sirisansaneeyakul, S., Vanichsriratana, W., Parakulsuksatid, P. 2021b. Two-step pretreatment of oil palm trunk for ethanol production by thermotolerent *Saccharomyces cerevisiae* SC90. Bioresour. Technol. 320: 124298. doi.org/10.1016/j.biortech.2020.124298

Tareen, A. K., Danbamrongtrakool, N., Sultan, I.N., Laemsak, N., Sirisansaneeyakul, S., Vanichsriratana, W., Parakulsuksatid, P. 2021c. Utilization of urea as a nitrogen source for ethanol production from oil palm trunk using simultaneous saccharification and fermentation. Agr. Nat. Resour. 55: 448–455. doi.org/10.34044/j.anres.2021.55.3.1

Tareen, A.K., Punsuvon, V., Parakulsuksatid, P. 2020a. Conversion of steam exploded hydrolyzate of oil palm trunk to furfural by using sulfuric acid, solid acid, and base catalysts in one pot. Energ. Source Part A. 4: 1741733. doi.org/10.1080/15567036.2020.1741733

Tareen, A.K., Punsuvon, V., Parakulsuksatid, P. 2020b. Investigation of alkaline hydrogen peroxide pretreatment to enhance enzymatic hydrolysis and phenolic compounds of oil palm trunk. 3 Biotech 10: 179. doi.org/10.1007/s13205-020-02169-6

Velmurugan, R., Muthukumar, K. 2012. Ultrasound-assisted alkaline pretreatment of sugarcane bagasse for fermentable sugar production: Optimization through response surface methodology. Bioresour. Technol. 112: 293–299. doi.org/10.1016/j.biortech.2012.01.168

Wang, F., Shi, D., Han, J., et al. 2020. Comparative study on pretreatment processes for different utilization purposes of switchgrass. ACS omega. 5: 21999–22007. doi.org/10.1021/acsomega.0c01047

Wan, C., Li, Y. 2010. Microbial pretreatment of corn stover with *Ceriporiopsis subvermispora* for enzymatic hydrolysis and ethanol production. Bioresour. Technol. 101: 6398–6403. doi: 10.1016/j.biortech.2010.03.070

Wilaithup, A., Sultan, I.N., Tareen, A.K., Laemsak, N., Sirisansaneeyakul, S., Vanichsriratana, W., Parakulsuksatid, P. 2022. Bioethanol production from oil palm trunk fibers using activated immobilized *Saccharomyces cerevisiae* SC90 under simultaneous saccharification and fermentation. Bioenerg. Res. 2022. doi.org/10.1007/s12155-021-10379-w

Woodham, C., Aryawan, A.A., Luke, S., Manning, P., Caliman, J., Naim, M., Turner, E., Slade, E. 2019. Effects of replanting and retention of mature oil palm riparian buffers on ecosystem functioning in oil palm plantations. Front. For. Glob. Chang 2: 29. doi.org/10.3389/ffgc.2019.00029

Wyman, C., Cai, C., Kumar, R. 2019. Bioethanol from lignocellulosic biomass. In: Kaltschmitt, M. (Ed.). Energy from Organic Materials (Biomass). Encyclopedia of Sustainability Science and Technology Series. Springer. New York, NY, USA. pp. 997–1022.

Xue, S., Nirmal, U., Bowman, J.M., David, C., Leonard, D.C.S., Bruce, E.D., Venkatesh, B. 2015. Sugar loss and enzyme inhibition due to oligosaccharide accumulation during high solids loading enzymatic hydrolysis. Biotechnol. Biofuels. 8: 195. doi.org/10.1186/s13068-015-0378-9

Yang, Y., Zhang, M., Wang, D. 2018. A comprehensive investigation on the effects of biomass particle size in cellulosic biofuel production. J. Energy Resour. Technol. 140: 041804. doi.org/10.1115/1.4039602

Yeh, A., Huang, Y.C., Chen, S.H. 2010. Effect of particle size on the rate of enzymatic hydrolysis of cellulose. Carbohyd. Polym. 79: 192–199. doi.org/10.1016/j.carbpol.2009.07.049

Zhao, X., Dong, L., Chen, L., Liu, D. 2013. Batch and multi-step fed-batch enzymatic saccharification of Formiline-pretreated sugarcane bagasse at high solid loadings for high sugar and ethanol titers. Bioresour. Technol. 135: 350–356. doi.org/10.1016/j.biortech.2012.09.074